

Magnetothermal Properties of Mesoscopic System Based on Ni₃Pt Nanoparticle

S. VOROBIOV^a, B. STROPKAI^a, M. KOŽEJOVÁ^a, O. TKACH^{a,b}, V. LATYSHEV^a,
E. ČIŽMÁR^a, M. ORENDÁČ^a AND V. KOMANICKÝ^{a,*}

^aInstitute of Physics, Faculty of Sciences, P.J. Šafárik University, Park Angelinum 9, 04013 Košice, Slovakia

^bFaculty of Electronics and Computer Technology, Sumy State University,
Rymyskyi-Korsakov Str. 2, 40007 Sumy, Ukraine

This article discusses the influence of the geometry of mesoscopic structures based on Ni₃Pt nanoparticles on the magnetothermal characteristics to maximize the magnetocaloric response. Nanostructured samples in the form of arrays of nanocylinders and nanowires were made using a combination of electron-beam lithography and electrochemical deposition methods. It was determined that the change from nanoparticles to nanostructured objects contributes to an increase in the magnetocaloric effect and change of the operating temperature range.

DOI: [10.12693/APhysPolA.137.922](https://doi.org/10.12693/APhysPolA.137.922)

PACS/topics: electron-beam lithography, electrochemical deposition, magnetocaloric effect

1. Introduction

Magnetocaloric cooling is a promising alternative to classical cooling methods due to its high environmental safety and energy efficiency. In this connection, the search for new magnetocaloric materials with high magnetocaloric response in the room temperature range, free from rare-earth elements is relevant [1]. Nanomaterials are potential candidates for usage in cooling systems when compared with bulk materials because their magnetic properties significantly depend on such effects as spin-disorder effects, the interaction between neighboring atoms, grains and particles, the crystal lattice structure, the texture, and the dimensional and surface effects [2, 3]. Changing these parameters may significantly influence the functional properties of these materials. Another equally important issue is the search for appropriate geometric schemes that would maximize magnetocaloric effect (MCE) [4]. In samples with a controlled microstructure of the sample (e.g., the formation of nanowires in an ordered matrix where distance between nanowires is controlled) it is possible to implement direct and inverse MCE, which is regulated by the magnetic field [5]. This is due to the superparamagnetic behavior of nanoobjects (e.g., nanowires, nanoparticles, nanodots) and induced magnetization axes (anisotropy). The use of commercially available nanoporous membranes such as nanoporous alumina imposes restrictions on nanoobject size and their geometric configuration. The solution to this problem is to use electron-beam lithography, which allows formation of arrays of nanoobjects in predetermined geometric arrangement with high accuracy. This paper presents the results of the investigations of the

magnetic properties of mesoscopic structures based on Ni₃Pt nanoparticles of different geometries, which were obtained by electrochemical deposition.

2. Experimental methods

The fabrication of various types of arrays (nanowires or cylindrical nanomagnets) based on Ni₃Pt nanoparticles was carried out using electron-beam lithography and electrochemical deposition method. Electron-beam lithography was used to form masks to resist further electrochemical deposition. Initially high-resolution positive resist for direct writing of e-beam polymethyl methacrylate (NANO 950 PMMA A, MicroChem) was spin-coated on glassy carbon substrates with the size of 0.5 × 0.5 mm². At the second stage, masks were filled with a resist by electrochemical deposition. The electrolyte solution for electrodeposition consisted of 0.003 mol/l K₂PtCl₄, 0.1 mol/l NiCl₂, and 0.5 mol/l NaCl [6]. The dimensions of the formed arrays were 2 × 2 mm² with a period between objects of 1 μm (distance between the centers of the objects). The prepared structures were characterized by scanning electron microscopy (SEM). The estimated number of defects in the obtained arrays that may occur due to substrate imperfections and limitations in an electrochemical deposition did not exceed 0.2%. We also determined the elemental composition after electrochemical deposition by energy dispersive X-ray spectroscopy (EDS) analysis. The results show that regardless of the geometry of the structures the deviation from the specified concentration does not exceed 1%.

The study of the phase state and crystal structure was carried out using the X-ray diffraction method (X-ray) and transmission electron microscopy (TEM), respectively. It was found that both nanoparticles and various types of arrays (nanowires, cylindrical nanomagnets) based on Ni₃Pt have a phase composition of fcc-Ni₃Pt,

*corresponding author

with an average crystallite size of $d_{aver} = 8$ nm. A more detailed discussion of the structural-phase analysis of structures based on Ni₃Pt nanoparticles was conducted by us in [7].

Thermomagnetic measurements of the samples in the zero-field-cooled (ZFC) and field-cooled (FC) regimes were performed using a commercial SQUID magnetometer (Quantum Design MPMS3) carried out in the temperature range 2–400 K. In order to evaluate magnetocaloric behavior, the measurement of the isothermal magnetization curves was conducted up to 0.5 T in the temperature range from 75 K to 400 K. The isothermal magnetic entropy change ΔS_M has been calculated using the Maxwell relation [8].

3. Results and discussion

The use of a combination of electron-beam lithography and electrochemical deposition gave us the opportunity to form nanostructured materials with precisely defined geometry and dimensions. Figure 1 shows the SEM image obtained from Ni₃Pt nanoparticles (Fig. 1a) and fragments of microstructures with different implemented geometry (Fig. 1b and c). The average size of Ni₃Pt nanoparticles was determined in the previous work [9] and was ≈ 130 nm. The average size of the nanostructured objects was determined using SEM analysis. Cylindrical nanomagnets (Fig. 1b) had height of $1.7 \mu\text{m}$ with a diameter of $0.35 \mu\text{m}$. The nanowires (Fig. 1c) had a length of $500 \mu\text{m}$ with a height of $1 \mu\text{m}$ and a width of $0.35 \mu\text{m}$. It should be noted that we consider nanowires, not in the classical sense (3D). The investigated “nanowires” are fixed on the substrate (2D). This configuration is more advantageous from the practical point of view since the objects of the structure can have controlled geometry and/or location.

The study of magnetic properties showed a significant difference in the thermomagnetic properties of Ni₃Pt nanoparticles with a random orientation on the sub-

strate and structures with a precisely defined geometry. Figure 2 shows the temperature dependence of the zero-field-cooled/field-cooled magnetization at 10 mT obtained from arrays of cylindrical nanomagnets (Fig. 2a) and nanowires (Fig. 2b) with two measurement geometries, the field was applied parallel and perpendicular to the matrix substrate (to the array substrate). The blocking temperature (T_B), which has been determined from the position of maximum in the temperature dependence of ZFC magnetization for Ni₃Pt nanoparticles is $T_B \approx 225$ K [9]. This value is significantly lower in comparison to the mesoscopic structures. Figure 2 shows $T_B \approx 300$ K for an array of cylindrical nanomagnets, while $T_B \approx 290$ K for an array of nanowires. A similar trend in the shift of blocking temperature was observed by other authors. For example, in [10], for Fe₃O₄ based nanoparticles, it was shown that agglomerated nanoparticles act as a cluster and have a higher T_B compared to “free” or individual nanoparticles. The temperature dependence of the magnetization obtained from the arrays of cylindrical nanomagnets remained almost unchanged (Fig. 2a) when the measurement geometry changed from parallel to perpendicular. A completely different situation is observed for nanowire arrays (Fig. 2b). ZFC-FC curves have a significant difference, which can be explained by the presence of magnetic anisotropy, which occurs due to the large length-to-diameter ratio of the nanowires [4].

Temperature dependence of the entropy change obtained for different types of structures with a field change of 0.5 T is shown in Fig. 3. The entropy change was studied for the parallel orientation. The results of the studies showed that the change in the entropy of the systems is very sensitive to a change in geometry. For example, in magnetic field of 0.5 T, for nanowires the maximum value of $-\Delta S_M = 0.05$ J/(kg K) is observed at $T_{max} = 350$ K, for cylindrical nanomagnets $-\Delta S_M = 0.13$ J/(kg K) at 360 K, and for nanoparticles Ni₃Pt the maximum value of $-\Delta S_M = 0.03$ J/(kg K) is observed at 270 K.

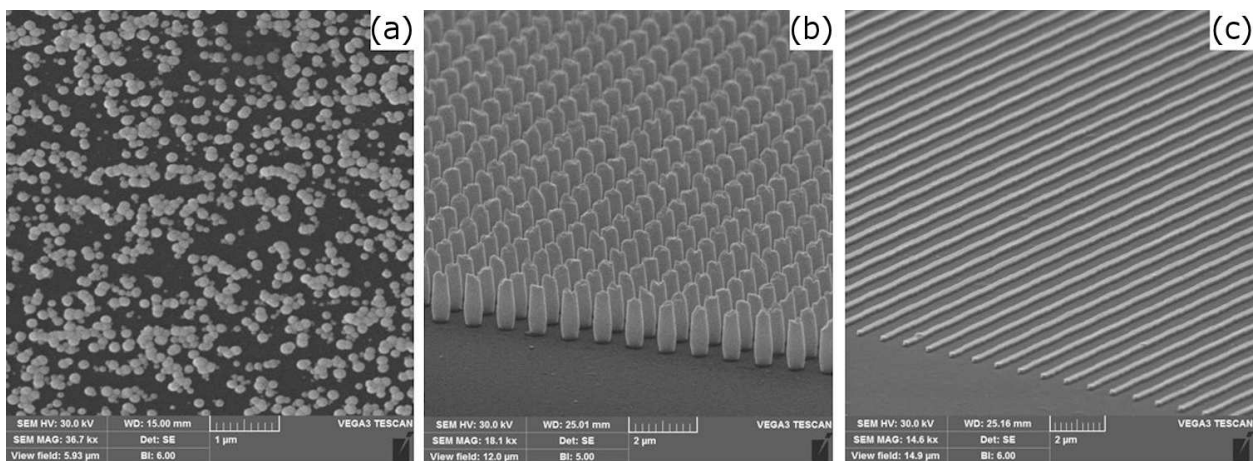


Fig. 1. SEM images of an array fragment of structures with a different geometry: (a) nanoparticles, (b) nanocylinders, (c) nanowires.

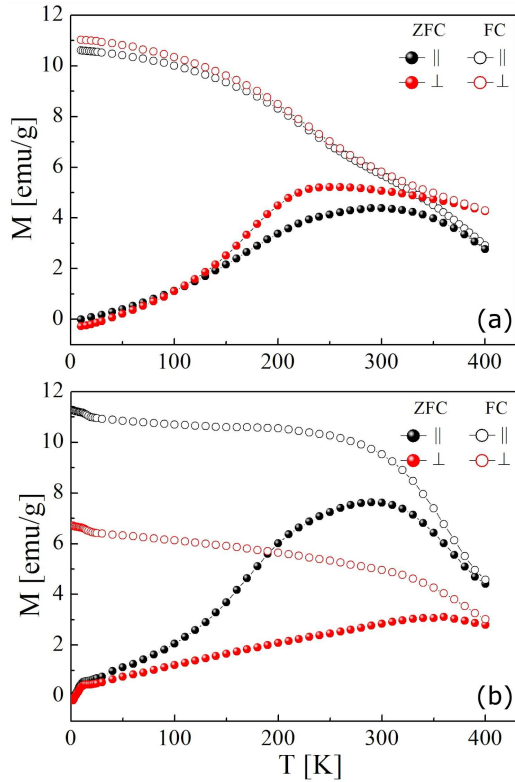


Fig. 2. (a) ZFC–FC curves obtained from arrays of cylinder nanomagnets, and (b) nanowires at a measuring field and cooling field of 10 mT.

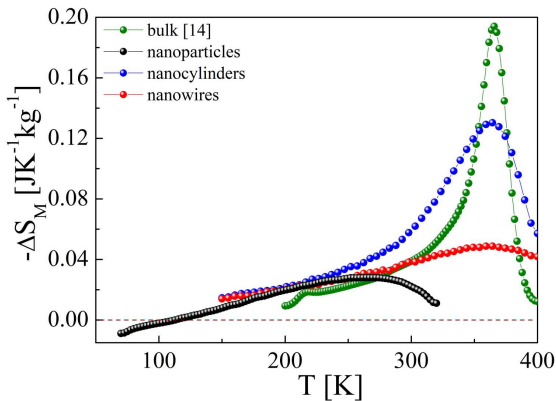


Fig. 3. Temperature dependence of the isothermal entropy change at magnetic field 0.5 T for different geometry of the structure.

The position of the maximum in the $-\Delta S_M(T)$ dependence becomes more noticeable for the arrays of nanostructures based on Ni₃Pt nanoparticles, as compared to nanoparticles, and the magnitude of the effect increases. For arrays of nanostructures based on nanoparticles, the maxima in the $-\Delta S_M(T)$ dependence correspond to the value of the bulk sample, although it should be noted that the maximum has a more specific shape for arrays of nanocylinders than for arrays of nanowires, which can be explained by different height of nanostructures. As was

shown in our previous work [7], for arrays of nanomagnets based on Ni₃Pt with the same parameters (height, chemical composition) a narrower maximum was observed for higher structures. At the same time, for nanoparticles, the maximum in temperature dependence of the isothermal entropy change has a diffused form, which is associated with the process of non-uniform blocking. This process can be explained by the wide size distribution of nanoparticles from 20 to 250 nm, which was shown in our previous work [10]. Magnetic moments of particles are blocked at certain temperatures. According to the Stoner–Wohlfarth model, the blocking temperature is defined as [11]:

$$T_B = \frac{KV}{k_B \ln(\tau_m/\tau_0)},$$

where k_B is the Boltzmann constant, V is the particle volume, K is the anisotropy constant, τ_m is the measuring time, and τ_0 is a characteristic constant of particles that it is related to gyromagnetic precession. Thus, the blocking temperature is directly proportional to the particle volume. Therefore, for nanoparticles with a certain dispersion, we see a superposition of the blocking temperature compared with nanostructured materials.

The maxima in the $-\Delta S_M(T)$ dependence correspond to the direct MCE associated with the magnetic transition from the ferromagnetic to the paramagnetic state. Although it should be noted that an inverse magnetocaloric effect is observed for Ni₃Pt nanoparticles at temperatures below 100 K. The presence of a direct and inverse magnetocaloric effect in systems of superparamagnetic nanoparticles was predicted by Monte Carlo simulations [12]. The calculations predict that the magnitude of inverse magnetocaloric effect depends both on the size and composition of the particles [12]. Since our sample contains certain number of particles with sizes less than 25 nm, which is very close to the critical size of Ni nanoparticles (24 nm) [13]. This might be why inverse magnetocaloric effect has been observed for this particular sample.

4. Conclusions

The arrays of mesoscopic objects with different geometries were formed on the basis of Ni₃Pt nanoparticles by the method of electron-beam lithography followed by electrochemical deposition. The study of the thermomagnetic characteristics showed that the change from nanoparticles to nanostructured objects shifts blocking temperature from 270 K for nanoparticles to ≈ 365 K for nanowires and nanocylinders. The magnitude of the magnetocaloric effect also increases significantly, and the peaks in the $-\Delta S_M(T)$ dependences become more pronounced. The maximum amplitude of the MCE was observed for arrays of nanocylinders at 0.5 T, ($-\Delta S_M$) = 0.13 J/(kg K), and 360 K. During the study of the temperature dependence of the entropy change in Ni₃Pt nanoparticles, the presence of an inverse magnetocaloric effect was observed.

Acknowledgments

This work has been supported by grant VEGA No. 1/0204/18, APVV-17-0059, APVV-14-0073 project PROMATECH, contract No. ITMS26220220186, and project NEMMA, contract No. ITMS: 313011T544. O. Tkach acknowledges the financial support provided by the National Scholarship Programme of the Slovak Republic (SAIA).

References

- [1] V. Chaudhary, X. Chen, R.V. Ramanujan, *Prog. Mater. Sci.* **100**, 64 (2019).
- [2] V. Franco, J.S. Blázquez, J.J. Ipus, J.Y. Law, L.M. Moreno-Ramírez, A. Conde, *Prog. Mater. Sci.* **93**, 112 (2018).
- [3] A. Elouafi, R. Moubah, S. Derkaoui, A. Tizliouine, R. Cherkaoui, S. Shi, A. Bendani, M. Sajieddine, H. Lassri, *Physica A* **523**, 260 (2019).
- [4] D. Serantes, V. Vega, W.O. Rosa, V.M. Prida, B. Hernando, M. Pereiro, D. Baldomir, *Phys. Rev. B* **86**, 104431 (2012).
- [5] V. Franco, K.R. Pirota, V.M. Prida, A.M.J.C. Neto, A. Conde, M. Knobel, B. Hernando, M. Vazquez, *Phys. Rev. B* **77**, 104434 (2008).
- [6] Y. Liu, C.M. Hangarter, U. Bertocci, T.P. Moffat, *J. Phys. Chem. C* **116**, 7848 (2012).
- [7] S. Vorobiov, D. Tomasova, V. Girman, H. You, E. Čižmár, M. Orendáč, V. Komanický, *J. Magn. Magn. Mater.* **474**, 63 (2019).
- [8] K.A. Gschneidner Jr., V.K. Pecharsky, A.O. Tsokol, *Rep. Prog. Phys.* **68**, 1479 (2005).
- [9] M. Kožejová, D. Hložná, Y. Hua Liu, K. Ráčzová, E. Čižmár, M. Orendáč, V. Komanický, *Acta Phys. Pol. A* **131**, 839 (2017).
- [10] D.K. Kim, Y. Zhang, W. Voit, K.V. Rao, M. Muhammed, *J. Magn. Magn. Mater.* **225**, 30 (2001).
- [11] M.C. Buján-Núñez, N. Fontaiña-Troitiño, C. Vázquez-Vázquez, M.A. López-Quintela, Y. Piñeiro, D. Serantes, D. Baldomir, J. Rivas, *J. Non-Cryst. Solids* **354**, 52222 (2008).
- [12] D. Baldomir, J. Rivas, D. Serantes, M. Pereiro, J.E. Arias, M.C. Bujan-Nunez, C. Vazquez-Vazquez *J. Non-Cryst. Solids* **353**, 790 (2007).
- [13] R. Das, A. Gupta, D. Kumar, S.H. Oh, S.J. Pennycook, A.F. Hebard, *J. Phys. Condens. Matter* **20**, 385213 (2008).